4,4′-Bismaleimidodiphenyl Methane Modified Novolak Resin/Titania Nanocomposites: Preparation and Properties

Guotao Lu, Ying Huang, Yehai Yan, Tong Zhao, Yunzhao Yu

Center for Molecular Sciences, Institute of Chemistry, Chinese Academy of Sciences, Beijing 100080, People's Republic of China

Received 22 June 2004; accepted 20 January 2005
DOI 10.1002/app.22116
Published online in Wiley InterScience (www.interscience.wiley.com).

ABSTRACT: 4,4′-Bismaleimidodiphenyl methane modified novolak resin/titania nanocomposites were prepared by the sol–gel process of tetrabutyl titanate in the presence of 4,4′-bismaleimidodiphenyl methane modified novolak resin prepolymers with acetyl acetone as a stabilizer. These nanocomposite materials were characterized by Fourier transform infrared analysis, dynamical mechanical analysis, thermogravimetric analysis, transmission electron microscopy, and field emission scanning electron microscopy. Nanometer titania particles were formed in the novolak resin matrix, and the average original particle size of the dispersed phase in the nanocomposites was less than 150 nm, but particle aggregates of larger size existed. The introduction of the titania inorganic phase with a nanoscale domain size did not improve the glass-transition temperature of the nanocomposites but lowered the thermal resistance of the material because of the incomplete removal of acetyl acetone coordinated with tetrabutyl titanate, and it improved the modulus of the material at lower temperatures (<200°C) but lowered the modulus at higher temperatures (>250°C). © 2006 Wiley Periodicals, Inc. J Appl Polym Sci 102: 52–57, 2006

Key words: nanocomposites; resins; thermal properties

INTRODUCTION

More and more interest has been shown in organic–inorganic nanocomposite (OINC) materials because of their wide and potential applications in electronics, optics, chemistry, and biomedicine.[1–4] Generally, the sol–gel method, which involves the hydrolysis and condensation reaction of metal alkoxides to produce glasses and ceramics at a relatively low temperature (usually <100°C), is a standard procedure used to prepare OINCs.[5] The advantages of the sol–gel method lie in the low temperature for synthesis, the ease of obtaining optically transparent nanocomposites, the versatility of control over the nature of the organic–inorganic interface, and the convenience of introducing new properties into the resulting materials.[5] To produce OINCs, soluble polymers or their monomers are usually introduced into the sol–gel system to provide the organic component in OINCs. Then, there are two approaches employed for the preparation of OINCs by the sol–gel process: nanoparticles of metal oxides or ceramics can be synthesized in the presence of a preformed polymer,[6–8] or sol–gel synthesis is carried out in an organic monomer that is polymerized subsequently or concurrently.[9–11] According to the interfacial nature of the resultant nanocomposites, OINCs can be divided into two classes: nanocomposites with interfacial covalent bonds between the organic and inorganic phases[12,13] and nanocomposites without covalent bonds between the two phases and with only hydrogen bonds between them.[14–16] Hybrid materials of polyacrylates,[17] polymethacrylates,[12] polyacrylonitrile,[7] polyvinylacetate,[15] polystyrene,[13] polycarbonate,[18] epoxy resin,[19] phenolic resin,[20] and polymaleimide[21] with SiO_2 or titania (TiO_2) nanoparticles have been studied.

Phenolic resins are of great interest because of their unique dimensional stability, good strength retention at high temperatures, high char yield, and flame retardatance.[22] In a previous article,[23] we reported the preparation of 4,4′-bismaleimidodiphenyl methane modified novolak resin (BMI-PN)/silica nanocomposites. Here we report the preparation of 4,4′-bismaleimidodiphenyl methane modified novolak resin/titania (BMI-PN/TiO_2) nanocomposites by the sol–gel process. Fourier transform infrared analysis (FTIR), dynamical mechanical analysis (DMA), thermogravimetric analysis (TGA), transmission electron microscopy (TEM), and field emission scanning electron microscopy (FESEM) were used to characterize the hybrid materials.

Compared to the precursor of SiO_2 [tetraethoxysilane (TEOS)], the precursor of TiO_2, tetrabutyl titanate [$Ti(O^nBu)_4$ or TBT], is much more reactive, and its hydrolysis rate is much higher than that of TEOS; this

Correspondence to: G. Lu, Chemistry Department, University of Missouri–Rolla, Rolla, MO 65401 (glrf8@umr.edu).

TABLE I
Composites of the BMI-PN/TiO_2 Nanocomposites

Sample	BMI-PN (%)	TiO_2 (%)
Cured BMI-PN	100	0
BMI-PN/Tit-2	98	2
BMI-PN/Tit-5	95	5

makes its aggregation much easier during the sol–gel process.[5] To overcome this problem, several methods have been developed to lower the hydrolysis rate of TBT: (1) adding organic acids or β-diketones such as acetyl acetone (AcAc) as chelating agents to coordinate with TBT and then reducing its hydrolysis rate;[24] (2) dropwise adding acidified water and alcohol into TBT to avoid aggregation;[25] (3) hydrolyzing without adding water, that is, using water in air (humidity = 60%) to slowly hydrolyze TBT;[26] and (4) using the inverse-adding method, that is, adding TBT to HCl-acidified water.[27] In this study, we used the first method to prepare the BMI-PN/TiO_2 nanocomposites.

EXPERIMENTAL

Materials

Phenol (CP) and formaldehyde (37% in water, CP) were acquired from Beijing Organic Chemicals Factory (Beijing, China) and were used as supplied. Allyl chloride was obtained from Qilu Petrochemical Co. (China) and was used after distillation. 4,4′-Bismaleimidodiphenyl methane (BMI) was purchased from Fenguang Chemical Co., Ltd. (China). It was a crystalline substance with a melting point of 151–154°C, and the purity was greater than 99%. TBT was a chemically pure reagent from Tianjian 2nd Chemicals Factory (Tianjian, China) and was used as supplied. AcAc, tetrahydrofuran (THF), and *n*-butanol (BuOH) were analytical reagents from the Beijing Chemical Factory (Beijing, China). THF was purified via refluxing over $Na/CO(C_6H_5)_2$ and distillation. Deionized water was acidified by hydrochloric acid (35–38%) to pH 2.

Synthesis of the BMI-PN prepolymers

The allylated phenol resins (APN) were prepared according to the literature.[22] The APN molecular weight was 1075 g/mol, the degree of allylation was 59.2%, as determined by ^{1}H-NMR, and the solid-state content was 88.2%. To synthesize BMI-PN, 36.59 g of APN (containing 0.15 mol of allyl groups) was charged in a three-necked flask and heated to 120°C. Then, 26.9 g of BMI (0.15 mol) was introduced. The reaction was continued for 1.5 h to give a transparent, red-brown BMI-PN prepolymer. The formation of BMI-PN was confirmed by FTIR and ^{1}H-NMR ($CDCl_3$) spectra.

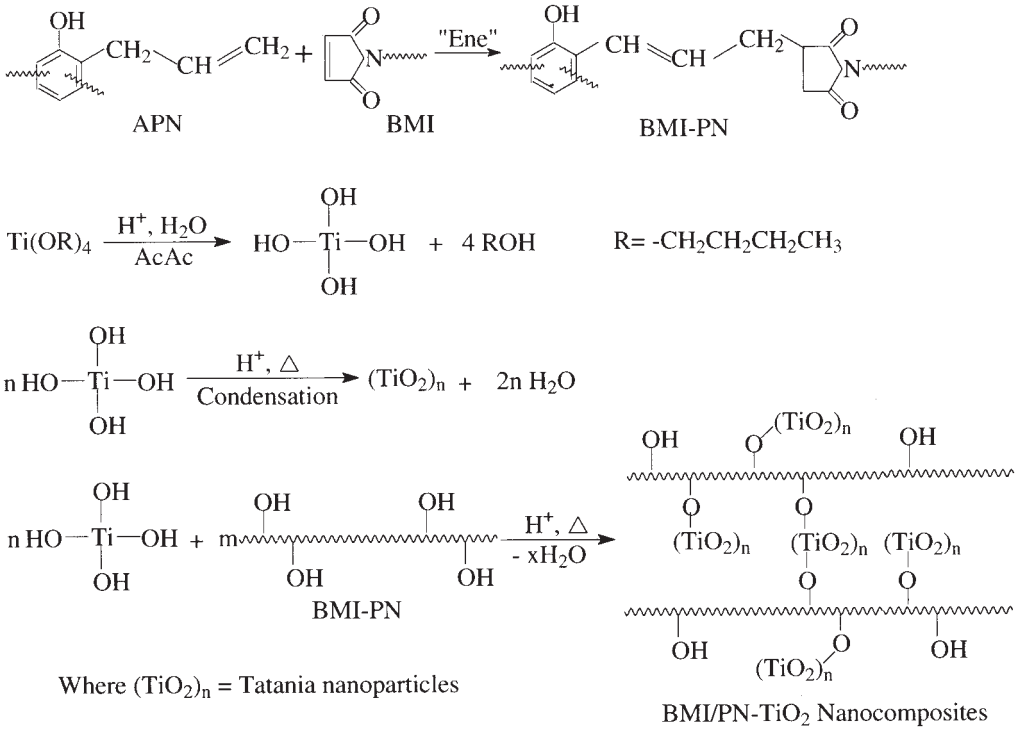

Figure 1 Reactions involved in the preparation of the BMI-PN/TiO_2 nanocomposites.

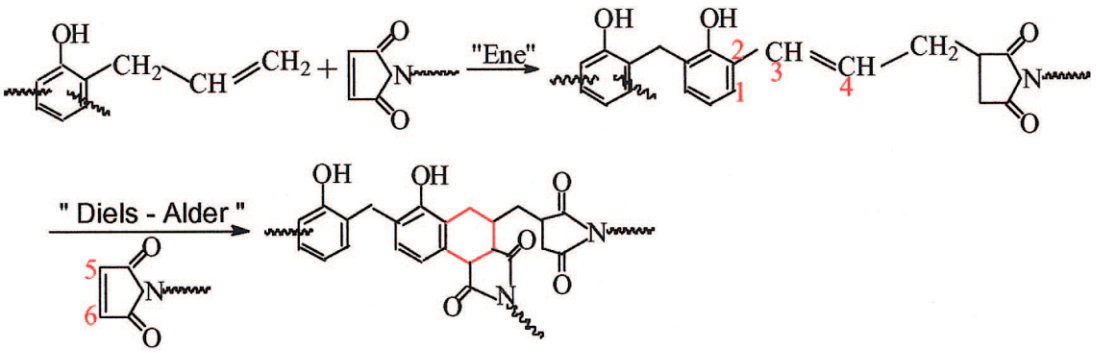

Figure 2 Reactions in the curing of BMI-PN. Carbons 1, 2, 3, 4, 5, and 6 were involved in the Diels–Alder reaction, and the new carbon ring that formed is shown in red. [Color figure can be viewed in the online issue, which is available at www.interscience.wiley.com.]

Synthesis of the BMI-PN/TiO_2 nanocomposites

BMI-PN/Tit-2 was prepared with the following procedure: 8.16 g of BMI-PN (allylation degree = 59.2%) was weighed into a three-necked, round flask equipped with a mechanical stirrer and a reflux condenser. Then, 6.23 g of THF was added to the flask, and the system was heated in an oil bath to keep the mixture's temperature at 80°C. After the prepolymer was dissolved completely, a clear mixture of 0.68 g of TBT and 0.3 g of AcAc was added to the solution, and at last 0.03 g of acidified water with pH 2.0 was added to the mixture to perform the sol–gel reaction. The reaction time was 1.5 h, and the system's temperature was kept at 80°C. Then, the volatile was removed at 50–130°C under reduced pressure to give the mold powder of the nanocomposite.

The specimens of the nanocomposites were prepared by compression molding. The curing cycle was 140°C/20 MPa/4 h + 200°C/20 MPa/6 h. The compositions of the BMI-PN/TiO_2 nanocomposites are listed in Table I.

Measurements

^{1}H-NMR spectra were obtained with a Bruker MW 300 spectrometer with $CDCl_3$ as a solvent. FTIR spectra were recorded on a PerkinElmer model 1600 IR spectrometer. DMA was performed on a PerkinElmer DMA-7 dynamical mechanical analyzer in the bending mode with the specimen dimensions of 15 mm × 4 mm × 1.5 mm. The measurements were conducted at 2 Hz from 40 to 350°C at a heating rate of 20°C/min. TGA was performed on a PerkinElmer TGA-7 thermogravimeter at a heating rate of 20°C/min under a nitrogen flow rate of 100 mL/min. The morphology of the BMI-PN/TiO_2 nanocomposite solution before curing was measured with a transmission electron microscope (JEM-200CX, JEOL). The microstructure features of the nanocomposite materials were examined with a Hitachi S-900 field emission scanning electron microscope. The fracture surfaces of the samples were coated with gold to eliminate charging effects, and a high voltage (10 kV) was used.

RESULTS AND DISCUSSION

Synthesis of the BMI-PN/TiO_2 nanocomposites

In the synthesis of the BMI-PN/TiO_2 nanocomposites, TBT was the resource of the inorganic phase. TBT was transformed into TiO_2 through hydrolysis and condensation, and the inorganic phase was linked with the resin matrix through ether groups produced by a condensation reaction during the curing process. The involved reactions are shown in Figures 1 and 2.

The process can be followed by IR spectroscopy. Shown in Figure 3(a,b) are the FTIR spectra of the BMI-PN prepolymer and the corresponding nanocomposite BMI-PN/Tit-2. There are new peaks at 670

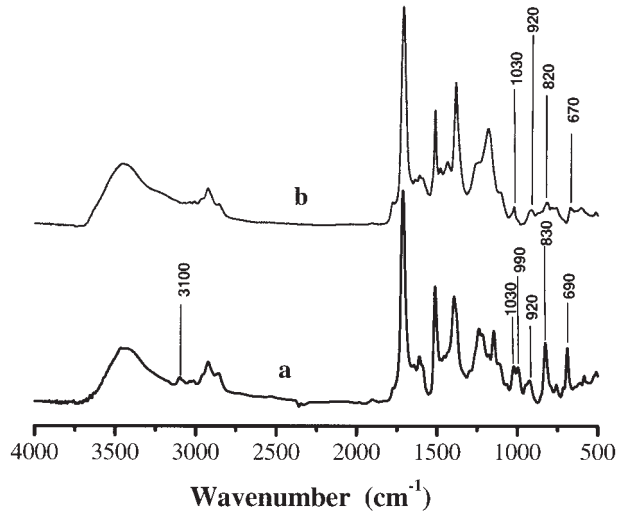

Figure 3 FTIR spectra for (a) cured BMI-PN and (b) the nanocomposite BMI-PN/Tit-2.

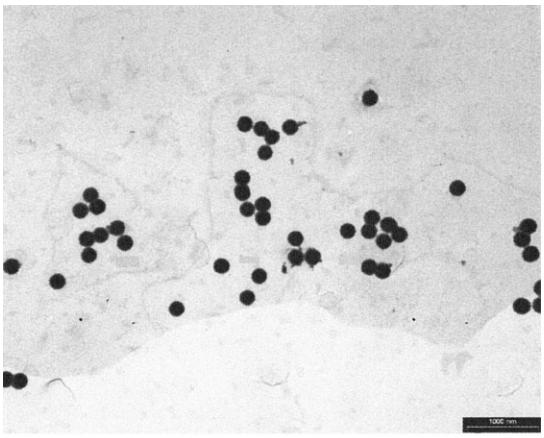

(a)

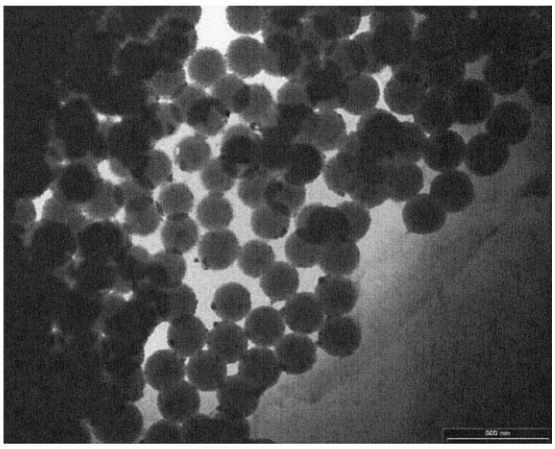

(b)

Figure 4 TEM photographs for the nanocomposite BMI-PN/Tit-2 solution before curing: (a) scale bar = 1000 nm and (b) scale bar = 500 nm.

cm^{-1} from Ti—O—Ti in TiO_2 and at 820 cm^{-1} from Ti—O—C in TiO_2.[28] These two peaks mean that there are TiO_2 particles formed in the BMI-PN matrix, whereas the presence of the Ti—O—C peak shows that the hydrolysis of TBT is not complete. The formation of TiO_2 nanoparticles can also be seen in Figure 4, the TEM photograph of the nanocomposite BMI-PN/Tit-2 solution before curing.

The reactions responsible for the curing of the resin are mainly the Ene reaction and the Diels–Alder reaction (Fig. 2). The proceeding of these reactions is indicated by the significant reduction of the absorptions at 3100, 990 (almost disappeared), and 920 cm^{-1} from the allyl groups. The formed crosslinking polymer network consists of the organic phase of the nanocomposites. A detailed discussion about the mechanism of the curing of the resin can be found in ref. 15.

Morphology of the BMI-PN/TiO_2 nanocomposites

TEM photographs of the BMI-PN/TiO_2 nanocomposite solution and FESEM photographs of the fracture surface of the BMI-PN/TiO_2 nanocomposites are shown in Figures 4 and 5, respectively. The TEM

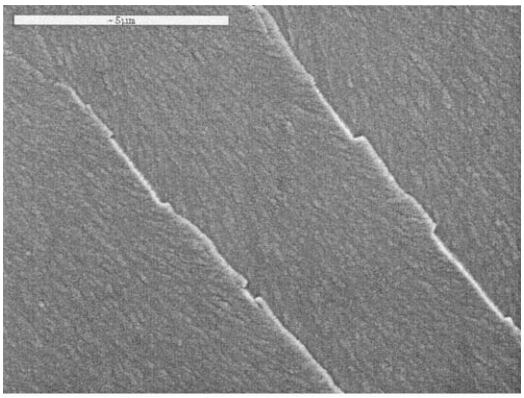

(a)

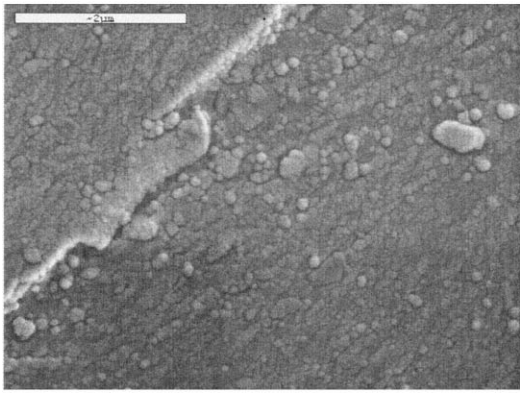

(b)

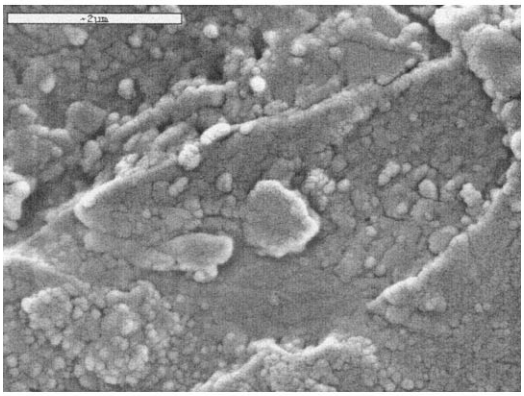

(c)

Figure 5 FESEM photographs of the BMI-PN/TiO_2 nanocomposites: (a) cured BMI-PN (scale bar = 5 μm), (b) BMI-PN/Tit-2 (scale bar = 2 μm), and (c) BMI-PN/Tit-5 (scale bar = 2 μm).

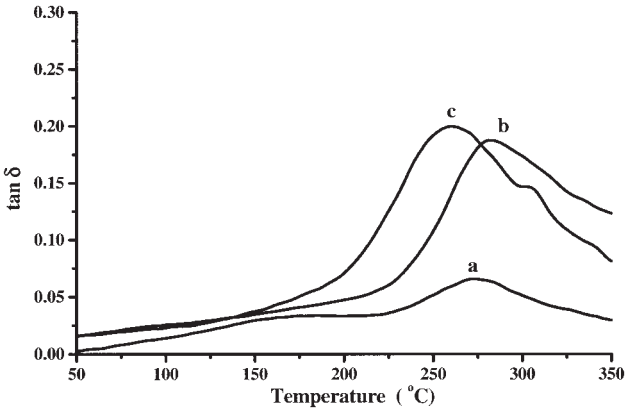

Figure 6 T_g of the BMI-PN/TiO_2 nanocomposites measured by DMA: (a) cured BMI-PN, (b) BMI-PN/Tit-2, and (c) BMI-PN/Tit-5.

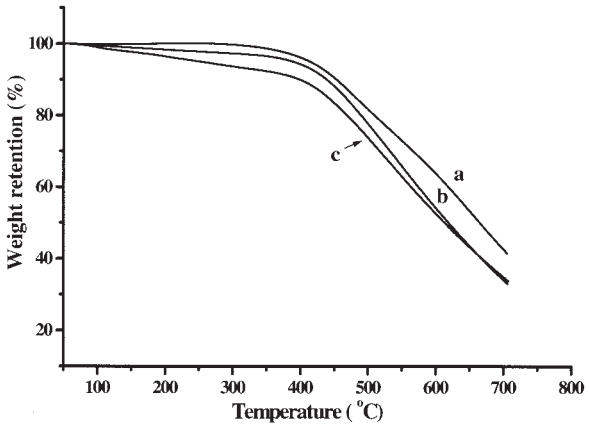

Figure 7 TGA diagrams for the BMI-PN/TiO_2 nanocomposites: (a) cured BMI-PN, (b) BMI-PN/Tit-2, and (c) BMI-PN/Tit-5.

micrograph shows that TiO_2 nanoparticles with a uniform size (ca. 150 nm) were formed in the BMI-PN/TiO_2 nanocomposite solution, and this is in good agreement with the FESEM studies. Figure 5 shows that the cured BMI-PN was a heterogeneous material, and phase separation was observed [Fig. 5(a)]. The origin of the phase separation has been discussed elsewhere.[29] The BMI-PN/TiO_2 nanocomposites were two-phase materials: the continuous phase was BMI-PN, and the dispersed phase consisted of TiO_2 nanoparticles [Fig. 5(b,c)]. The average original particle size of the dispersed phase in the BMI-PN/TiO_2 nanocomposites was about 150 nm, with particle aggregates of larger sizes with increasing inorganic content [Fig. 5(b,c)].

Thermal properties of the BMI-PN/TiO_2 nanocomposites

The glass-transition temperatures (T_g's) of the BMI-PN/TiO_2 nanocomposites were characterized by DMA, as shown in Figure 6 and Table II. Figure 6 shows that the incorporation of TiO_2 nanoparticles had no obvious effect in improving the T_g's of the nanocomposites. However, the introduction of TiO_2 facilitated the curing process, and the phase separation of the BMI-PN resin in the nanocomposites disappeared. The proposed mechanism is that AcAc, which was added to the system as the chelating agent of TBT, did not decompose completely during the *in situ* hydrolysis, condensation, and curing process. The presence of AcAc thus increased the compatibility between BMI and APN and facilitated the crosslinking and curing reactions between them; it then caused the formation of a higher crosslinked, homogeneous network of organic phases. Therefore, the phase separation disappeared.

TGA diagrams of the BMI-PN/TiO_2 nanocomposites with different inorganic phase contents are shown in Figure 7. There were two stages in the weight-loss process of the nanocomposites. The elimination of water formed by the condensation of residual Ti—OH groups accounted for the minor weight loss beginning at ~150°C. The major weight loss occurred beyond 450°C, and it was due to the decomposition of the organic polymer in these BMI-PN/TiO_2 nanocomposites. Table III summarizes the temperatures for 5% weight loss and 10% weight loss and the temperatures at the maximum decomposition rate (T_{max}'s) of the BMI-PN/TiO_2 nanocomposites in the TGA diagrams.

The introduction of the inorganic phase into the nanocomposites lowered the temperatures for 5% weight loss and 10% weight loss, T_{max}, and the weight retention at 700°C of the resin. The probable reason is

TABLE II
T_g of the BMI-PN/TiO_2 Nanocomposites Measured by DMA

Sample	T_g (°C) First	T_g (°C) Second
Cured BMI-PN	175.2	275.3
BMI-PN/Tit-2	281.0	
BMI-PN/Tit-5	259.3	

TABLE III
Thermal Resistance of the BMI-PN/TiO_2 Nanocomposites

Sample	5 wt % loss temperature (°C)	10 wt % loss temperature (°C)	T_{max} (°C)	Weight retention (%)
Cured BMI-PN	415.4	452.9	655.5	42.5
BMI-PN/Tit-2	390.3	438.4	540.6	35.9
BMI-PN/Tit-5	252.8	398.9	519.9	35.8

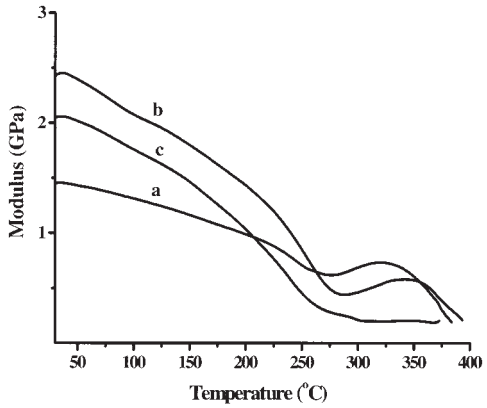

Figure 8 Modulus–temperature diagrams of the BMI-PN/TiO_2 nanocomposites measured by DMA: (a) cured BMI-PN, (b) BMI-PN/Tit-2, and (c) BMI-PN/Tit-5.

that in the nanocomposites there were no covalent bonds between the organic phases and inorganic phases (although in some cases, nanocomposites without covalent bonds between organic and inorganic phases may have better thermal resistance than the polymer matrix[14–16]), and the remaining AcAc catalyzed the decomposition process of the organic phase.

Figure 8 shows the change in the storage modulus with the temperature for BMI-PN, BMI-PN/Tit-2, and BMI-PN/Tit-5. The introduction of the TiO_2 phase improved the moduli of the nanocomposites at lower temperatures (<200°C) but lowered the moduli at higher temperatures (>250°C). The aforementioned explanation for the decrease in the thermal resistance also holds true for this phenomenon.

CONCLUSIONS

BMI-PN/TiO_2 nanocomposites were prepared from BMI-PN prepolymers by the sol–gel process. The TiO_2 particles were formed through the hydrolysis and condensation of TBT. The average diameter of the primary particles of the dispersed phase was about 150 nm, but there existed particle aggregates. The introduction of the TiO_2 inorganic nanophase did not enhance the T_g's of the nanocomposites but lowered the thermal resistance of the material because of the incomplete decomposition of AcAc coordinated with TBT; it improved the modulus of the material at lower temperatures (<200°C) but lowered the modulus of the material at higher temperatures (>250°C).

References

1. MacLachlan, M. J.; Manners, I.; Ozin, G. A. Adv Mater 2000, 12, 675.
2. Ellsworth, M. W.; Gin, D. L. Polym News 1999, 24, 331.
3. Hench, L. L.; West, J. K. Chem Rev 1990, 90, 33.
4. Novak, B. M. Adv Mater 1993, 5, 422.
5. Wen, J.; Wilkes, G. Chem Mater 1996, 8, 1667.
6. Deng, C.; James, P. F.; Wright, P. V. J Mater Chem 1998, 8, 153.
7. Wei, Y.; Yang, D. C.; Tang, L. G. Makromol Chem Rapid Commun 1993, 14, 273.
8. Shojaie, S. S.; Rials, T. G.; Kelley, S. S. J Appl Polym Sci 1995, 58, 1263.
9. Schmidt, H. J Non-Cryst Solids 1989, 112, 419.
10. Ellsworth, M. W.; Novak, B. M. J Am Chem Soc 1991, 113, 1756.
11. Novak, B. M.; Davis, C. Macromolecules 1991, 24, 5481.
12. Sunkara, H. B.; Jethmalani, J. M.; Ford, W. T. Chem Mater 1994, 6, 362.
13. Mourey, T. H.; Miller, S. M.; Wesson, J. A.; et al. Macromolecules 1993, 25, 45.
14. Pope, E. J.; Asami, M.; Mackenzie, J. D. J Mater Res 1989, 4, 1017.
15. Landry, C. J.; Coltrain, B. K. J Macromol Sci Pure Appl Chem 1994, 31, 1965.
16. Morikawa, A.; Yamaguchi, H.; Kakimoto, M.; Imai, Y. Chem Mater 1994, 6, 913.
17. Wei, Y.; Wang, W.; Yang, D.; Tang, L. Chem Mater 1994, 6, 1737.
18. Landry, C. J. T.; Coltrain, B. K. Polym Prepr 1990, 32, 514.
19. Messersmith, B.; Giannelis, E. P. Chem Mater 1994, 6, 1719.
20. Haragguchi, K.; Usami, Y. Chem Lett 1997, 51.
21. Lu, G. T.; Huang, Y. J Mater Sci 2002, 37, 2305.
22. Yan, Y. H.; Shi, X. M.; Liu, J.; Zhao, T.; Yu, Y. Z. J Appl Polym Sci 2002, 83, 1651.
23. Lu, G. T.; Huang, Y.; Yan, Y. H.; Zhao, T.; Yu, Y. Z. J Polym Sci Part A: Polym Chem 2003, 41, 2599.
24. Judeinstein, P.; Sanchez, C. J Mater Chem 1996, 6, 511.
25. Wang, B.; Wilkes, G. L. J Polym Sci Part A: Polym Chem 1991, 29, 905.
26. Mauritz, K. A. J Appl Polym Sci 1990, 40, 1401.
27. Wang, B.; Wilkes, G. L. J Macromol Sci Pure Appl Chem 1994, 31, 249.
28. Deng, D. S.; James, P. F.; Wright, P. V. J Mater Chem 1998, 8, 153.
29. Lu, G. T.; Huang, Y.; Yan, Y. H.; Zhao, T.; Yu, Y. Z. Polym Mater Sci Eng 2002, 87, 330.